European Journal of Pharmacology 700 (2013) 201–209

Contents lists available at SciVerse ScienceDirect

European Journal of Pharmacology

journal homepage: www.elsevier.com/locate/ejphar

Cardiovascular pharmacology

Infliximab prevents increased systolic blood pressure and upregulates the AKT/eNOS pathway in the aorta of spontaneously hypertensive rats

Ademir Gazzoto Filho [a], Andrezza Kinote [a], Daniel J. Pereira [a], André Rennó [a], Rodrigo C. dos Santos [a], Silvia E. Ferreira-Melo [b], Licio A. Velloso [b], Silvana Bordin [c], Gabriel F. Anhê [a], Heitor Moreno Junior [b,*]

[a] Department of Pharmacology, Faculty of Medical Sciences, State University of Campinas, Campinas, SP, Brazil
[b] Department of Internal Medicine, Faculty of Medical Sciences, State University of Campinas, Campinas, SP, Brazil
[c] Department of Physiology and Biophysics, Institute of Biomedical Sciences, State University of Sao Paulo, Sao Paulo, SP, Brazil

ARTICLE INFO

Article history:
Received 21 January 2012
Received in revised form
9 November 2012
Accepted 20 November 2012
Available online 7 December 2012

Keywords:
Infliximab
Hypertension
Insulin resistance
TNFα
eNOS

ABSTRACT

High systolic blood pressure caused by endothelial dysfunction is a comorbidity of metabolic syndrome that is mediated by local inflammatory signals. Insulin-induced vasorelaxation due to endothelial nitric oxide synthase (eNOS) activation is highly dependent on the activation of the upstream insulin-stimulated serine/threonine kinase (AKT) and is severely impaired in obese, hypertensive rodents and humans. Neutralisation of circulating tumor necrosis factor-α (TNFα) with infliximab improves glucose homeostasis, but the consequences of this pharmacological strategy on systolic blood pressure and eNOS activation are unknown. To address this issue, we assessed the temporal changes in the systolic pressure of spontaneously hypertensive rats (SHR) treated with infliximab. We also assessed the activation of critical proteins that mediate insulin activity and TNFα-mediated insulin resistance in the aorta and cardiac left ventricle. Our data demonstrate that infliximab prevents the upregulation of both systolic pressure and left ventricle hypertrophy in SHR. These effects paralleled an increase in AKT/eNOS phosphorylation and a reduction in the phosphorylation of inhibitor of nuclear factor-κB (Iκβ) and c-Jun N-terminal kinase (JNK) in the aorta. Overall, our study revealed the cardiovascular benefits of infliximab in SHR. In addition, the present findings further suggested that the reduction of systolic pressure and left ventricle hypertrophy by infliximab are secondary effects to the reduction of endothelial inflammation and the recovery of AKT/eNOS pathway activation.

1. Introduction

Recent studies have demonstrated that insulin resistance, endothelial dysfunction and vascular inflammation play important roles in the aetiology of hypertension. Insulin resistance, a key event in the pathophysiology of type 2 diabetes mellitus, is characterised by an inappropriate response of peripheral organs to insulin (DeFronzo, 2010). The disruption of intracellular insulin signal transmission is related to insulin resistance in such way that several possible molecular mechanisms have been described to impair insulin-induced glucose uptake by skeletal muscles and adipose tissue in diabetic patients (Cnop et al., 2011).

In addition to its role in glucose homeostasis, insulin is an important mediator of vasorelaxation through a mechanism that involves endothelium-dependent nitric oxide (NO) production (Scherrer et al., 1994). Insulin-mediated NO generation by endothelial cells results from the upstream activation of the insulin-stimulated serine/threonine kinase (AKT) pathway (Zeng et al., 2000). AKT leads to the direct activation of endothelial NO synthase (eNOS) by phosphorylating serine 1177 of eNOS (Dimmeler et al., 1999).

Endothelial dysfunction is thought to play an important role in the genesis of hypertension by increasing vascular tone and blood pressure (Desjardins and Balligand, 2006). Therefore, endothelial insulin resistance and the subsequent impairment of insulin-induced vasorelaxation through stimulation of NO synthesis are being investigated as relevant mechanisms for diabetes-related vascular dysfunction (Lee et al., 2009; Yang et al., 2009). Importantly, activation of the insulin-induced AKT/eNOS pathway is impaired in the aorta of spontaneous hypertensive rats (SHR) (Zecchin et al., 2003).

Tumor necrosis factor-α (TNFα) is an inflammatory cytokine produced in rats that are both insulin resistant and hypertensive (Espinola-Klein et al., 2011). Several studies have indicated that TNFα action is a key factor in insulin resistance in peripheral insulin-sensitive tissues and endothelial dysfunction (de Alvaro et al., 2004). Recent studies have reported that infliximab, a TNFα-neutralising antibody, effectively restores AKT activity in

* Corresponding author. Tel.: +55 19 3521 9538; fax: +55 19 3289 2968.
E-mail address: hmoreno@uol.com.br (H.M. Junior).

0014-2999
http://dx.doi.org/10.1016/j.ejphar.2012.11.059

both the skeletal muscle and the liver of insulin-resistant rodents, thus improving glucose homeostasis (Araújo et al., 2007; Barbuio et al., 2007).

The present study was designed to assess the putative effects of infliximab treatment on AKT and eNOS phosphorylation in the aortas of SHR. In addition, we investigated the effects of infliximab on the systolic blood pressure levels and left ventricle hypertrophy that are characteristic of this animal model of hypertension.

2. Materials and methods

2.1. Experimental design

Male Wistar Kyoto rats (WKY) and spontaneous hypertensive rats (SHR) weighing 200–250 g were obtained from the Central Animal House Services (CEMIB) of the State University of Campinas. These animals were divided into six groups ($n=10$): WKY receiving water as vehicle (WKY+veh), WKY receiving 1.5 mg/kg/week infliximab (WKY+inflix 1.5), WKY receiving 6 mg/kg/week infliximab (WKY+inflix 6), SHR receiving water as vehicle (SHR+veh), SHR receiving 1.5 mg/kg/week infliximab (SHR+inflix 1.5) and SHR receiving 6 mg/kg/week infliximab (SHR+inflix 6). s.c. injections of infliximab or vehicle were performed once a week beginning when the animals were 8 weeks old. All animals were kept on a strict light/dark-cycle (12-h light, 12-h dark) with free access to food and water. All of the experiments described in this manuscript were approved by the Committee for Ethics in Animal Experimentation (CEEA) located in the Institute of Biology of the State University of Campinas. The CEEA guidelines are in accordance with the NIH Guide for the Care and Use of Laboratory Animals and with the ethical guidelines established by the Brazilian College for Animal Experimentation (COBEA).

2.2. Insulin tolerance test (ITT) and glucose tolerance test (GTT)

The animals were fasted for 12 h before the ITT and GTT. The ITT was performed by injecting insulin (2 IU/kg) i.p., and blood samples were collected from the tail at 0 min, 5 min, 10 min, 15 min, 20 min, 25 min and 30 min for the determination of blood glucose levels. The constant rate for glucose disappearance (K_{ITT}) was calculated using the following formula: $K_{ITT}=0.693/\text{half-time}$. The glucose half-time of glucose decay was calculated from the slope of the least-square analysis of the blood glucose concentrations during the linear decay phase.

The GTT was performed by i.p. glucose injection (2 g/kg of a 20% solution of D-glucose). Blood samples were collected from the tail at 0 min, 10 min, 15 min, 30 min, 60 min and 120 min for the determination of blood glucose levels. The area under the curve (AUC) of glycaemia vs. time was calculated above each individual baseline (basal glycaemia) to estimate glucose tolerance.

For both the GTT and ITT, blood glucose was measured using an Accu-Chek Active glucometer and the appropriate test strips (Roche Diagnostics, Basel, Switzerland).

2.3. Non-invasive (tail-cuff) blood pressure and body weight measurements

Blood pressure was assessed using the tail-cuff method with a noninvasive blood pressure system (CODAHT41EA, Kent Scientific Corporation, Torrington, Connecticut, USA). Systolic blood pressure levels of the WKY and SHR treated with either vehicle or infliximab were measured twice a week throughout the study, and the mean of these two measurements was determined.

The rats were placed in a holder for three consecutive days (15 min per day) prior to beginning blood pressure measurements. On the day of blood pressure measurements, the rats were confined in small, dark holders for 10 min to 15 min prior to obtaining pressure measurements. Before and during these measurements, the holders were placed over warming pads (Far Infrared Stasis Technology, Kent Scientific Corporation, Connecticut, USA). Body temperature and heart rate were monitored throughout the blood pressure measurements, and no changes were observed in these parameters during the procedure.

2.4. Echocardiography

After 8 weeks of treatment with infliximab or vehicle, the rats were subjected to a transthoracic echocardiographic study under anaesthesia with intraperitoneal injection of ketamine HCl (10 mg/kg) and xylazine (10 mg/kg). Two-dimensional and M-mode echocardiogram images were obtained at the papillary muscle level using an echocardiographic system equipped with an 11.5-MHz phased array transducer. The left ventricular volume and ejection fraction were calculated using the single-plane prolate ellipsoid geometric model from the parasternal long-axis view. Two independent, blinded investigators performed echocardiographic studies with a commercially available Siemens Acuson CV70 echo-scanner (Siemens Aktiengesellschaft—Munich, Bavaria, Germany) with a mutifrequency sector transducer (2–4 MHz) placed on the shaved left hemithorax of the rats. The M-mode measurements included end-diastolic septal thickness, end-diastolic posterior thickness, left-ventricular end-systolic and end-diastolic diameters, left ventricular ejection fraction, left ventricular mass, left ventricular mass index and relative wall thickness. The heart rate was also recorded.

The left ventricular ejection fraction and left ventricular mass were calculated as follows: ([{left-ventricular end diastolic diameter^3 – left-ventricular end systolic diameter^3}/left-ventricular end systolic diameter^3] × 100) and $0.8 \times \{1.04 \times [(\text{interventricular septal wall thickness} + \text{posterior wall thickness} + \text{left-ventricular end diastolic diameter})^3 - (\text{left-ventricular end diastolic diameter}^3)]\} + 0.6$, respectively. The mass values were obtained in grams. Digital data of 10 consecutive heart cycles were recorded and transferred to a personal computer work-station for off-line analysis (Brown et al., 2002; Watson et al., 2004). The left ventricular mass index was obtained by normalising the left ventricular mass to the body weight.

2.5. Histological analysis

After 8 weeks of treatment, the rats were euthanised and the heart was removed and fixed in 10% formalin for 24 h. Subsequently, the atria were removed, and the left ventricle was carefully separated from the right ventricle and cut into four equal rings perpendicular to the long axis of the heart. The tissue samples were subsequently processed using routine histological methods. Briefly, tissues were sectioned (5 μm), stained with hematoxylin–eosin and analysed by light microscopy. For each rat ($n=5$), twenty fields of view of each section were randomly studied by light microscopy (Leica Q500 iW Leica DMLS, Leica Imaging Systems, Cambridge, UK).

All fields of view (1600 per group) were captured with a digital camera to produce amplified images (40 ×), which were analysed with commercial software (Quantimet 500, Cambridge Instruments, Cambridge, UK). The heart samples were coded and then assessed by two independent, blinded observers.

2.6. Protein extraction and western blot

Rats were anaesthetised with sodium thiopental (100 mg/kg body wt). Once, anaesthesia was ascertained by the loss of pedal reflex, the thoracic cavity was opened and the thoracic aorta was

removed and homogenised in SDS lysis buffer (10% sodium dodecyl sulphate, 100 mM Tris (pH 7.4), 10 mM EDTA, 10 mM sodium pyrophosphate, 100 mM sodium fluoride, 10 mM sodium vanadate) with a Polytron PTA 20S generator (model PT 10/35; Brinkmann Instruments, Inc., Westbury, NY) operated at maximum speed for 30 s. The left ventricle was also removed and processed for protein extraction. The extracts were processed, subjected to SDS-PAGE (10% bis-acrylamide) and electrotransferred to a nitrocellulose membrane as previously described (Caperuto et al., 2008). Nonspecific protein binding to nitrocellulose was reduced by preincubating the membranes overnight at 4 °C in blocking buffer (5% non-fat dried milk, 10 mm Tris, 150 mm NaCl, and 0.02% Tween-20). After blocking, the nitrocellulose membranes were incubated with primary antibodies. Anti-phospho-AKT (Ser 473), anti-Iκβ, anti-AKT 1/2/3, anti-phospho-JNK (Thr 183/Tyr 185) and anti-TNFα were purchased from Santa Cruz Biotechnology (Santa Cruz, CA, USA). Anti-phospho-Iκβ (Ser 32) was purchased from Cell Signalling Technology (Beverly, MA, USA). Anti-phospho-eNOS (Ser 1177), anti-eNOS and anti-β-actin were obtained from Millipore. Bound antibodies were detected with horseradish peroxidase-conjugated anti-IgG and visualised by chemiluminescence with X-ray-sensitive films. Band intensities were quantified from the developed autoradiographs using the Scion Image program.

2.7. Caspase-3 processing

Caspase-3 processing was determined after detection of caspase-3 and Pro-caspase-3 by western blotting with a polyclonal antibody (Cat. No. sc1225; Santa Cruz Biotechnology, Santa Cruz, CA, USA). After optical densitometry analysis, the values of caspase-3 were normalised to those of Pro-caspase-3.

2.8. Statistical analyses

The results are presented as the mean ± S.E.M. Comparisons were performed using a one-way ANOVA, with Tukey–Kramer post-test (INStat; Graph Pad Software, Inc., San Diego, CA) and the unpaired Student's t test when appropriate. The level of significance was set at $P<0.05$.

3. Results

3.1. Infliximab increases glucose tolerance and insulin sensitivity and decreases systolic pressure in SHR

Initially, we wanted to determine whether infliximab would modulate glucose tolerance in WKY and SHR rats (Fig. 1A and B). By analysing the AUC, we found that rats in the SHR+veh group displayed no changes in glucose tolerance compared to those of the WKY+veh group. Infliximab treatment improved glucose tolerance exclusively in the SHR independent of the dose (values of SHR+inflix 1.5 and SHR+inflix 6 were 51% and 57% lower than that of SHR+veh, respectively; $P<0.05$) (Fig. 1C). Fasting glycaemia was unaltered by infliximab treatment in both WKY and SHR (Fig. 1D). In agreement with previous data (Zecchin et al., 2003), we found that insulin sensitivity was decreased in rats in the SHR+veh group compared to those of the WKY+veh group (to 47% of WKY+veh values; $P<0.05$). Infliximab treatment increased insulin sensitivity in rats of the SHR+inflix 6 group compared to those of the SHR+veh group (to 249% of SHR+veh values; $P<0.05$) (Fig. 1E).

No changes in body weight were detected during the treatment period, resulting in a similar final body weight among the groups (Fig. 2A and B). Infliximab did not alter systolic blood pressure in WKY (Fig. 2C). In contrast, infliximab treatment induced a progressive decrease in systolic blood pressure in SHR. This decrease in systolic blood pressure was detected as early as the end of the sixth week of treatment. Thus, at the end of the sixth week, systolic blood pressure was significantly reduced in the rats in the SHR+inflix 1.5 and SHR+inflix 6 groups compared with those in the SHR+veh group (22% and 21% lower than SHR+veh values, respectively; $P<0.05$). The reduction in systolic pressure induced by infliximab was detected up to the eighth week of treatment in the SHR+inflix 1.5 and SHR+inflix 6 groups (41% lower than SHR+veh values; $P<0.05$) (Fig. 2D).

3.2. Infliximab increases AKT and eNOS phosphorylation in the aorta of SHR

Reduced activation of the AKT/eNOS pathway is suggested to contribute to increased blood pressure values in SHR (Zecchin et al., 2003). Thus, the next step of our investigation was to assess whether infliximab would modulate AKT/eNOS pathway in the aorta of SHR. We found that the aortas of the SHR+veh rats displayed reduced levels of AKT phosphorylation compared to those of WKY+veh rats (63% lower than WKY+veh values $P<0.05$). Infliximab treatment increased the level of AKT phosphorylation compared to that observed in the SHR+veh group (values of SHR+inflix 1.5 and SHR+inflix 6 were 97% and 86% higher than those of SHR+veh, respectively; $P<0.05$). AKT phosphorylation in the aortas of WKY was not modulated by infliximab (Fig. 3B). The total AKT levels were unaltered among the groups and were used to normalise the values of phosphorylated AKT.

In addition, our data show that eNOS phosphorylation is reduced in the aortas of SHR+veh rats (71% lower than WKY+veh values; $P<0.05$). Treatment with infliximab increased the levels of eNOS phosphorylation compared to the levels observed in rats in the SHR+veh group (values of SHR+inflix 1.5 and SHR+inflix 6 were 171% and 236% higher, respectively, than those of SHR+veh; $P<0.05$). Phosphorylation of eNOS in the aortas of WKY was not affected by infliximab (Fig. 3D). The total eNOS levels were unaltered among the groups and were used to normalise the values of phosphorylated eNOS.

3.3. Infliximab reduces TNFα expression and activity of inflammatory pathways in the aorta of SHR

Increased endothelial JNK and NFκB pathways activation is reported to occur in SHR (Sugita et al., 2004; Sanz-Rosa et al., 2005). The increased activity of these pathways prompted us to evaluate whether the infliximab-induced changes in AKT/eNOS pathway were associated with modulation of inflammatory pathways. Our data demonstrated that JNK phosphorylation was 143% higher in the aortas of rats in the SHR+veh group compared to the aortas of rats in the WKY+veh group ($P<0.05$). Infliximab reduced JNK phosphorylation in the aortas of rats in the SHR+inflix 1.5 and SHR+inflix 6 groups (to 48% and 22% of the SHR+veh values, respectively; $P<0.05$). Interestingly, the higher dose of infliximab promoted an increase in JNK phosphorylation in the aortas of WKY (134% higher than WKY+veh; $P<0.05$) (Fig. 3F). The phosphorylation levels of JNK were normalised to those of β-actin.

The phosphorylation levels of Iκβ, a direct target of IκK, were not significantly different when comparing the aortas of WKY+veh rats to those of SHR+veh rats. Treatment with infliximab reduced the phosphorylation of Iκβ in the aortas of rats in the SHR+inflix 1.5 and SHR+inflix 6 groups (to 48% and 42% of SHR+veh values, respectively; $P<0.05$) but did not alter Iκβ phosphorylation in the aortas of WKY (Fig. 3E). Total Iκβ levels were used to normalise the values of phosphorylated Iκβ.

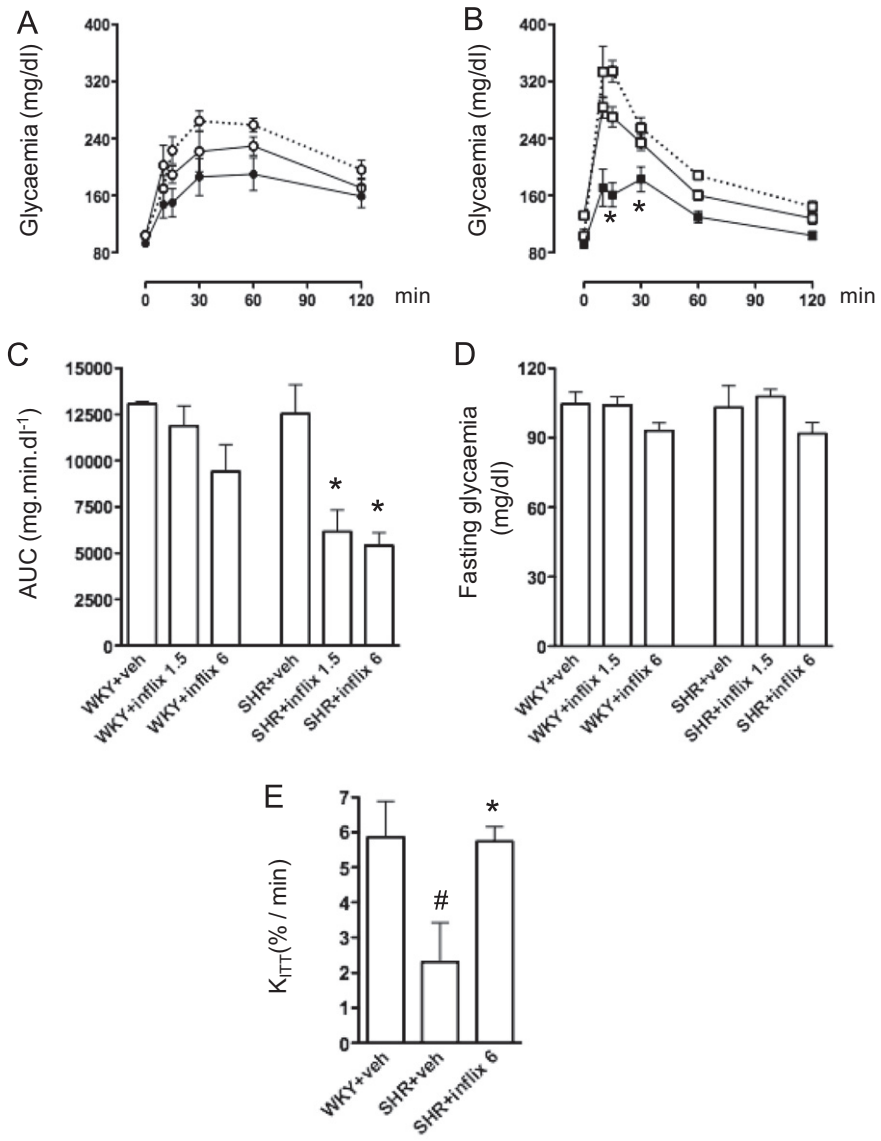

Fig. 1. Glucose tolerance, insulin sensitivity and fasting glycaemia in WKY and SHR treated with infliximab. WKY and SHR treated with vehicle or infliximab for 8 weeks were subjected to a glucose tolerance test ((A) and (B), respectively). The AUC of each animal was calculated using the individual baseline (C). Twelve-hour fasting glycaemia was determined prior to glucose challenge (D). To estimate insulin sensitivity, K_{ITT} was calculated using glycaemia values acquired during the ITT (E). The dotted line with open circles represents the WKY+veh group, the solid line with open circles represents the WKY+inflix 3 group, the solid line with closed circles represents the WKY+inflix 6 group, the dotted line with open squares represents the SHR+veh group, the solid line with open squares represents the SHR+inflix 3 group and the solid line with closed squares represents the SHR+inflix 6 group. The data are presented as the mean ± S.E.M. *$P < 0.05$ vs. SHR+veh; #$P < 0.05$ vs. WKY+veh.

TNFα expression was 62% lower in the SHR+veh group compared to that of the WKY+veh group. In agreement with the reductions in JNK and Iκβ phosphorylation, we also found that infliximab reduced TNFα expression in the aortas of SHR (values of TNFα levels in SHR+inflix 1.5 and SHR+inflix 6 were 66% and 96% lower, respectively, than those of SHR+veh; $P < 0.05$). Similarly, infliximab reduced TNFα expression in the aortas of WKY (values of WKY+inflix 1.5 and WKY+inflix 6 were 22% and 39% lower, respectively, than those of WKY+veh; $P < 0.05$) (Fig. 3C). The values for TNFα expression were normalised to those of β-actin.

3.4. Infliximab reduces cardiac hypertrophy and does not interfere with ventricular function in SHR

To assess if the reduction in blood pressure following infliximab treatment is correlated with an impairment of ventricular function caused by infliximab (Anker and Coats, 2002), we next investigated the cardiac tissue of WKY and SHR treated with either vehicle or infliximab. Echocardiography of untreated and infliximab-treated WKY and SHR rats (8 weeks of treatment) revealed no differences in heart rate, ejection fraction and left-ventricular end-systolic and end-diastolic diameters at different infliximab doses. Although its effect was not dose dependent, infliximab reduced end-diastolic septal wall thickness, end-diastolic posterior wall thickness, relative wall thickness, left ventricle mass and left ventricle mass index in SHR. Consistent with this echocardiographic finding, histometric analysis showed that infliximab reduced the diameters of cardiomyocytes in SHR. We also found that left ventricle mass, left ventricle mass index, relative wall thickness and cardiomyocyte diameters were increased in rats of the SHR+veh group compared to those of the WKY+veh group (Table 1).

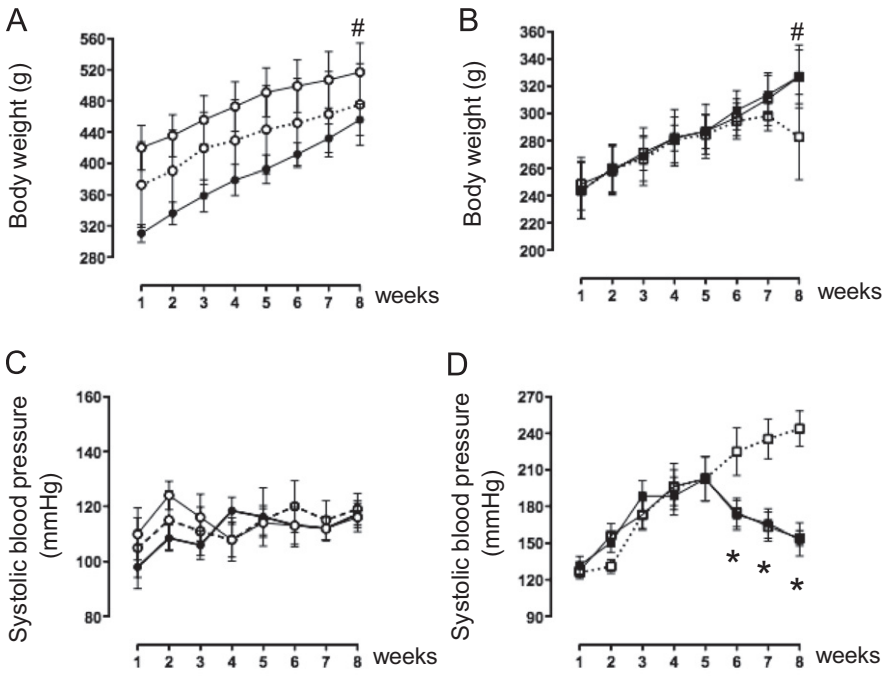

Fig. 2. Body weight and systolic blood pressure in WKY and SHR during infliximab treatment. The body weights of WKY and SHR treated with vehicle or infliximab ((A) and (B), respectively) and the systolic blood pressure ((C) and (D), respectively) were measured weekly after the first week until the end of the eighth week of treatment. The dotted line with open circles represents the WKY+veh group, the solid line with open circles represents the WKY+inflix 3 group, the solid line with closed circles represents the WKY+inflix 6 group, the dotted line with open squares represents the SHR+veh group, the solid line with open squares represents the SHR+inflix 3 group and the solid line with closed squares represents the SHR+inflix 6 group. The data are presented as the mean ± S.E.M. #$P<0.05$ vs. the same group at the first week; *$P<0.05$ vs. SHR+veh at the same time point.

3.5. *Infliximab reduces AKT phosphorylation and caspase-3 processing in the left ventricle of SHR*

Our analysis of cardiac parameters revealed that JNK phosphorylation, although elevated in the left ventricle of SHR+veh rats (89% higher than in WKY+veh; $P<0.05$), was not modulated by infliximab in the WKY and SHR groups (Fig. 4B). Cardiac TNFα expression was similar in the WKY+veh and SHR+veh groups and was not modulated by infliximab in the SHR group. However, higher doses of infliximab stimulated TNFα expression in the left ventricle (71% higher than WKY+veh; $P<0.05$) (Fig. 4C).

Iκβ phosphorylation was increased in the left ventricle of SHR+veh rats (412% higher than in WKY+veh; $P<0.05$). Treatment with infliximab did not alter Iκβ phosphorylation in WKY but reduced this phosphorylation in SHR (the values in SHR+inflix 1.5 and SHR+inflix 6 were 47% and 71% lower, respectively, than in SHR+veh; $P<0.05$) (Fig. 4D).

AKT phosphorylation was increased in the left ventricle of SHR+veh rats (15% higher than in WKY+veh; $P<0.05$). Infliximab treatment, however, reduced AKT phosphorylation in the left ventricles of SHR (values in SHR+inflix 1.5 and SHR+inflix 6 were 21% and 42% lower than in SHR+veh, respectively; $P<0.05$) but not in those of WKY (Fig. 4E).

To assess putative changes in cell death within the cardiac tissue, we analysed caspase-3 processing, a hallmark of cellular apoptosis. Our data show that caspase-3 processing was reduced in the left ventricles of rats in the SHR+inflix 6 group (to 31% of SHR+veh values; $P<0.05$) (Supplementary Fig. 1).

4. Discussion

The present investigation revealed that an 8-week treatment with infliximab was able to reduce systolic pressure levels and left ventricular hypertrophy in spontaneously hypertensive rats. This is the first demonstration that the use of infliximab, often administered to normotensive patients, can result in cardiovascular benefits in a rodent model of spontaneous hypertension. The mechanism that we suggest to explain this effect was based on previous reports regarding the use of infliximab in obese/hypertensive patients. The use of infliximab in subjects with metabolic syndrome results in a potentiation of the vasodilatation induced by insulin during a hyperinsulinemic/euglycaemic clamp (Tesauro et al., 2008). Importantly, these results obtained by Tesauro et al. (2008) demonstrated that the effect of infliximab was dependent on NO synthesis. In addition, sera that were obtained from patients with Crohn's disease who were treated with infliximab induced increased eNOS expression when added to human umbilical vein endothelial cells (Altorjay et al., 2011). Our data also show that infliximab did not alter blood pressure values in normotensive WKY rats.

Based on these previous studies of infliximab, we sought to correlate the improvement in systolic pressure induced by infliximab in SHR with secondary changes in pathways involved in vascular relaxation. Phosphorylation of eNOS at serine 1177 facilitates NO production by this enzyme (Dimmeler et al., 1999). Notably, a reduction in eNOS activity is known to be involved in the hypertensive state of SHR (Chou et al., 1998). Consistent with the published information, our data show that eNOS phosphorylation is reduced in the aorta of SHR. Moreover, we found that infliximab increased eNOS phosphorylation in the aorta of SHR.

Reduced eNOS and AKT phosphorylation are simultaneously present in the aorta of SHR (Zecchin et al., 2003). Because AKT, a canonical substrate of insulin signalling, is an important upstream effector that targets eNOS serine phosphorylation (Dimmeler et al., 1999) we next assessed whether changes in AKT phosphorylation would correlate with the effects of infliximab on eNOS phosphorylation. Our data revealed that AKT phosphorylation

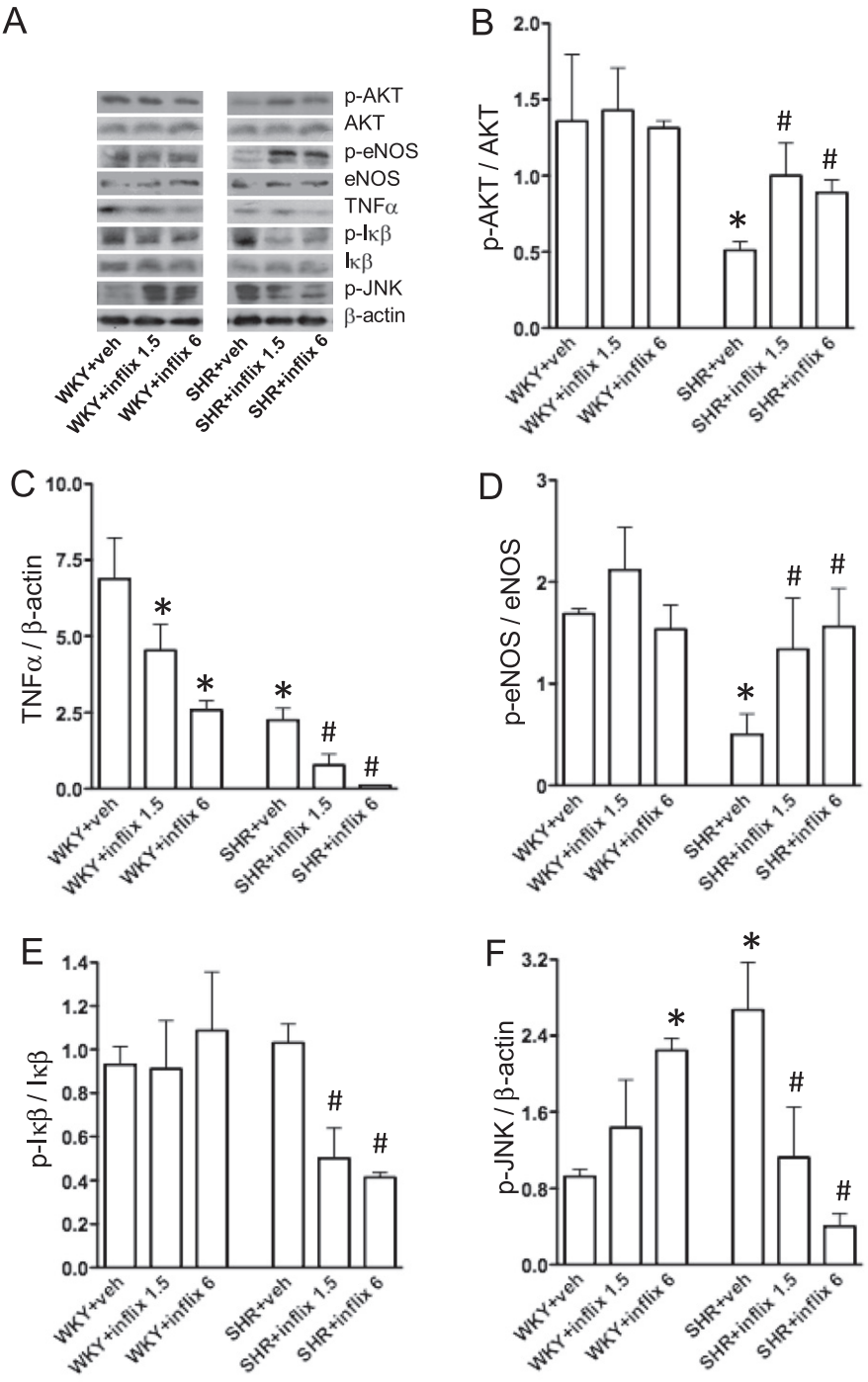

Fig. 3. AKT/eNOS activation and inflammatory pathways in the aorta of WKY and SHR treated with infliximab. The aortas were removed from WKY and SHR treated with either vehicle or infliximab for 8 weeks, and samples were prepared for western blot detection of phospho-AKT, AKT, phospho-eNOS, eNOS, TNFα, phospho-Iκβ, Iκβ, phospho-JNK and β-actin (A). Values of phospho-AKT were normalised to total AKT (B). Values of TNFα were normalised to β-actin (C). Values of phospho-eNOS were normalised to total eNOS (D). Values of phospho-Iκβ were normalised to total Iκβ (E). Values of phospho-JNK were normalised to β-actin (F). The data are presented as the mean ± S.E.M. $^{*}P < 0.05$ vs. WKY+veh; $\#P < 0.05$ vs. SHR+veh.

was reduced in the aorta of vehicle-treated SHR but was increased after infliximab treatment. These data are in accordance with previous publications that demonstrated that infliximab increases AKT phosphorylation in insulin-sensitive peripheral tissues (Araújo et al., 2007; Barbuio et al., 2007).

Published data support the hypothesis that infliximab-induced upregulation of the AKT/eNOS pathway is likely due to the neutralising properties upon circulating TNFα. In support of this hypothesis, TNFα signalling through the NF-κB pathway was described to contribute to endothelial dysfunction in obese mice (Yang et al., 2009, AJP). Moreover, TNFα production by small arteries is able to mediate a reduction in NO-dependent relaxation (Virdis et al., 2011).

After establishing that the effect of infliximab on SHR correlates with upregulation of the AKT/eNOS pathway in the aorta and with a reduction of systolic blood pressure, we analysed putative changes in TNFα signalling that are associated with abrogation

Table 1
Echocardiographic parameters and cardiomyocyte diameter in WKY and SHR after 8 weeks of treatment either with vehicle or infliximab.

	WKY+veh	WKY+inflix 1.5	WKY+inflix 6.0	SHR+veh	SHR+inflix 1.5	SHR+inflix 6.0
Heart rate (bpm)	403 ± 27.4	389 ± 24.3	400 ± 26.4	395 ± 29.6	394 ± 30.1	409 ± 28.3
End-diastolic septal wall thickness (mm)	0.1280 ± 0.026	0.1290 ± 0.037	0.1300 ± 0.034	0.1540 ± 0.004	0.1260 ± 0.002[b]	0.1380 ± 0.008[b]
End-diastolic posterior wall thickness (mm)	0.1380 ± 0.004	0.1360 ± 0.004	0.1400 ± 0.003	0.1660 ± 0.004	0.1240 ± 0.003[b]	0.1420 ± 0.002[b]
Left ventricular end diastolic diamenter (cm)	0.5920 ± 0.0140	0.6940 ± 0.0461	0.7020 ± 0.0454	0.5820 ± 0.0233	0. 5740 ± 0.02288	0.5960 ± 0.0331
Left ventricular end-systolic diamenter (cm)	0.3360 ± 0.0081	0.3200 ± 0.0104	0.3780 ± 0.0376	0.3160 ± 0.0261	0.3140 ± 0.0156	0.3160 ± 0.0261
Left ventricular ejection fraction (%)	82 ± 1.8	82 ± 1.3	84 ± 1.9	83 ± 2.1	83 ± 2.1	83 ± 4.9
Left ventricle mass (mg)	973 ± 26.0	977 ± 28.4	1078 ± 41.1	1051 ± 39.8[a]	909 ± 20.4[a,b]	983 ± 27.1[a,b]
Left ventricle mass index (mg/g)	2.25 ± 0.08	2.24 ± 0.21	2.05 ± 0.16	3.15 ± 0.17[a]	2.91 ± 0.06[a,b]	2.58 ± 0.05[a,b]
Relative wall thickness	0.467 ± 0.016	0.436 ± 0.022	0.392 ± 0.030	0.552 ± 0.015[a]	0.478 ± 0.019[a,b]	0.481 ± 0.052[a,b]
Cardiomyocyte diameter (μm)	17.3 ± 0.54	18.2 ± 0.73	17.8 ± 0.75	32.9 ± 0.65[a]	24.8 ± 0.62[a,b]	23.1 ± 0.48[a,b]

[a] $P < 0.01$ vs. WKY+veh, WKY+inflix 1.5 and WKY+inflix 6.0.
[b] $P < 0.05$ vs. SHR+veh.

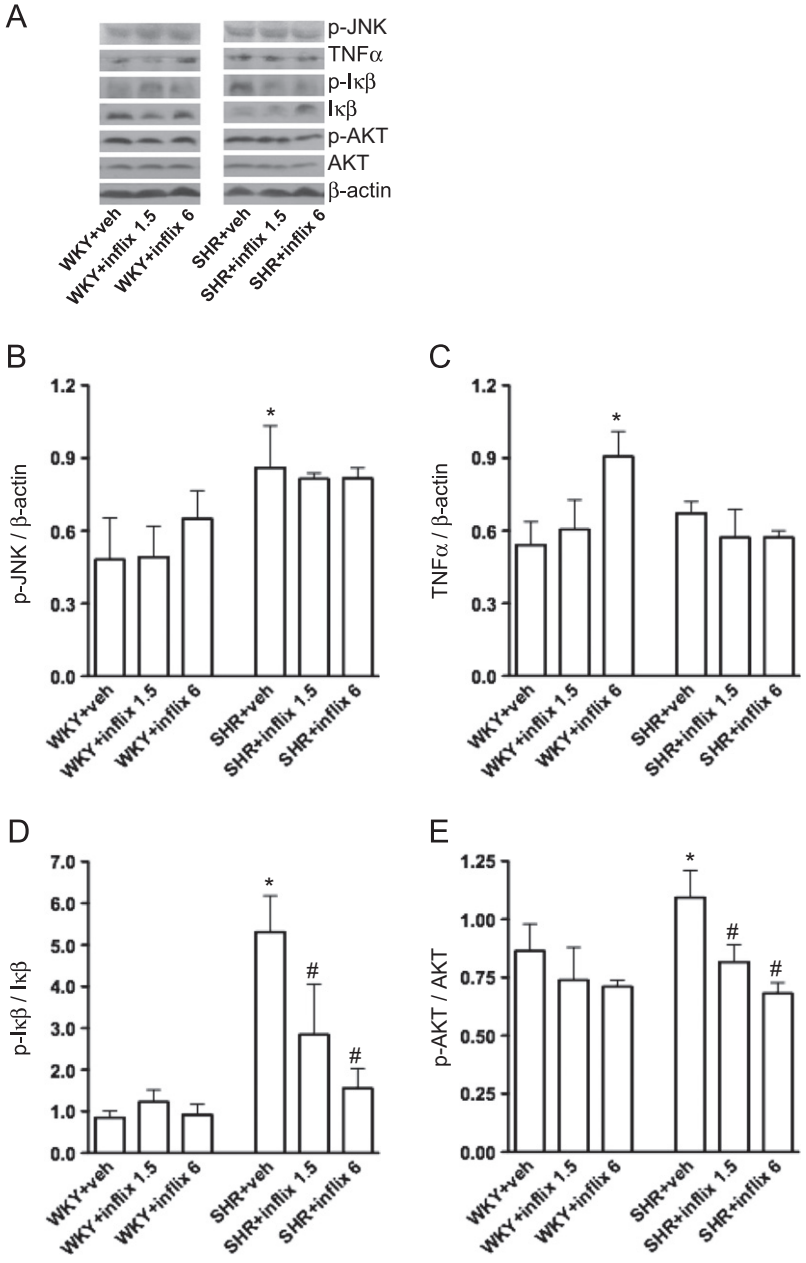

Fig. 4. AKT/eNOS activation and inflammatory pathways in the left ventricle of WKY and SHR treated with infliximab. The left ventricles were removed from WKY and SHR treated with vehicle or infliximab for 8 weeks, and samples were prepared for western blot detection of phospho-AKT, AKT, TNFα, phospho-Iκβ, Iκβ, phospho-JNK and β-actin (A). Values of phospho-JNK were normalised to β-actin (B). Values of TNFα were normalised to β-actin (C). Values of phospho-Iκβ were normalised to total Iκβ (D). Values of phospho-AKT were normalised to total AKT (E). The data are presented as the mean ± S.E.M. *$P < 0.05$ vs. WKY+veh; #$P < 0.05$ vs. SHR+veh.

of AKT activation. AKT is classically activated by several endogenous ligands that bind to transmembrane receptors with intrinsic tyrosine kinase activity. Thus, insulin receptor tyrosine phosphorylation and subsequent tyrosine phosphorylation of substrates that serve as docking platforms, such as IRS, are the initial rate-limiting steps for insulin-mediated AKT activation. Recently, evidence has emerged demonstrating the importance of IRS serine phosphorylation in blunting insulin-receptor-mediated IRS tyrosine phosphorylation, which leads to a reduction in insulin-induced AKT activation and, by extension, insulin resistance (Taniguchi et al., 2006).

Convincing studies have reported that increased serine phosphorylation of IRS is the most reliable mechanism through which chronic, subclinical inflammation causes insulin resistance in obese animals and humans (Paz et al., 1997). Several circulating factors can modulate IRS serine phosphorylation in insulin-sensitive tissues, but TNFα, produced by adipose tissue, plays a critical role (Kanety et al., 1995). Two serine/threonine kinases activated by TNFα, c-Jun N-terminal Kinase (JNK) and inhibitor of NF-κB kinase (IκK), are known to mediate IRS serine phosphorylation and insulin resistance (Taniguchi et al., 2006).

In addition, TNFα was shown to cause insulin resistance and to reduce eNOS activation in endothelial progenitor cells (Chen et al., 2011). Importantly, TNFα-induced impairment of eNOS activation was described to be dependent on IκK and JNK in the arteries of ob/ob mice (Yang et al., 2009). In concordance with these reports, we found that infliximab reduced both Iκβ and JNK phosphorylation in the aortas of SHR. Because TNFα expression is positively regulated by NF-κB activity (Messer et al., 1990), the present results showing that infliximab decreases TNFα expression in the aorta of hypertensive rats further corroborates the proposition that this drug reduces the activity of the IκK/Iκβ/NF-κB pathway in aortic tissue. Furthermore, other anti-hypertensive pharmacological approaches were described to decrease TNFα expression and NF-κB activity in the aorta of SHR (Sanz-Rosa et al., 2005). Interestingly, vehicle-treated SHR had lower levels of TNFα in the aorta compared to vehicle-treated WKY. Thus, it is possible that TNFα produced by the adipose tissue acts in the aorta of SHR, where it contributes to elevated blood pressure. We believe that the reduction in TNFα that was observed in the aorta of SHR after infliximab treatment is a consequence of negative regulation of the NF-κB and JNK pathways due to TNFα neutralisation.

To determine whether the reduction in systolic blood pressure induced by infliximab correlated with changes in left ventricular function, we assessed various echocardiographic parameters in SHR and WKY. Upon comparing these groups, we found no differences in left ventricular systolic or diastolic function. In contrast, left ventrivle mass index and cardiomyocyte diameter were clearly reduced in SHR treated with infliximab. In agreement with these data, it has been shown that increasing pressure induced by aortic constriction is able to stimulate left ventricle hypertrophy, which is attenuated by eNOS activation (Bhuiyan et al., 2009). Thus, we hypothesise that infliximab-induced upregulation of the AKT/eNOS pathway in the aorta increases vascular relaxation and, consequently, reduces pressure overload-induced ventricle hypertrophy in SHR. Further supporting this hypothesis, eNOS knockout mice are known to display increased systolic blood pressure and left ventricle hypertrophy (Yang et al., 1999).

In contrast to what we observed in the aorta, AKT phosphorylation was decreased in the left ventricle of infliximab-treated rats. One possible explanation for these differential effects of infliximab may be that pressure overload is a key stimulator of AKT activation in the left ventricle that leads to ventricle hypertrophy (Ha et al., 2005). Therefore, we believe that the reduction in cardiac AKT activation by infliximab is secondary to upregulation of endothelial AKT/eNOS. This adaptation would reduce left ventricle hypertrophy in SHR.

Because AKT activation is implicated in the inhibition of apoptosis, favouring cell survival in many cell types, we assessed caspase-3 processing in the cardiac tissue of infliximab-treated rats. We found that infliximab treatment actually reduced caspase-3 processing in the left ventricle of SHR, which strongly suggests that this drug does not induce apoptosis in the left ventricle despite a decrease in AKT phosphorylation.

In summary, our data demonstrate that neutralisation of circulating TNFα by infliximab reduces systolic blood pressure in hypertensive rats. This reduction is associated with upregulation of AKT/eNOS in the aorta. In addition, we demonstrate that upregulation of the AKT/eNOS pathway in the aorta correlates with reduced arterial TNFα expression and Iκβ and JNK activation. This adaptation most likely results in indirect reduction of left ventricle hypertrophy and cardiac AKT activation.

Acknowledgements

The authors acknowledge Fundação de Amparo a Pesquisa do Estado de São Paulo (FAPESP) and Conselho Nacional de Desenvolvimento Científico e Tecnológico (CNPq) for financial support.

Appendix A. Supporting information

Supplementary data associated with this article can be found in the online version at http://dx.doi.org/10.1016/j.ejphar.2012.11.059.

References

Altorjay, I., Veréb, Z., Serfozo, Z., Bacskai, I., Bátori, R., Erdodi, F., Udvardy, M., Sipka, S., Lányi, Á., Rajnavölgyi, É., Palatka, K., 2011. Anti-TNF-alpha antibody (infliximab) therapy supports the recovery of eNOS and VEGFR2 protein expression in endothelial cells. Int. J. Immunopathol. Pharmacol. 24, 323–335.

Anker, S.D., Coats, A.J., 2002. How to RECOVER from RENAISSANCE? The significance of the results of RECOVER, RENAISSANCE, RENEWAL and ATTACH. Int. J. Cardiol. 86, 123–130.

Araújo, E.P., De Souza, C.T., Ueno, M., Cintra, D.E., Bertolo, M.B., Carvalheira, J.B., Saad, M.J., Velloso, L.A., 2007. Infliximab restores glucose homeostasis in an animal model of diet-induced obesity and diabetes. Endocrinology 148, 5991–5997.

Barbuio, R., Milanski, M., Bertolo, M.B., Saad, M.J., Velloso, L.A., 2007. Infliximab reverses steatosis and improves insulin signal transduction in liver of rats fed a high-fat diet. J. Endocrinol. 194, 539–550.

Bhuiyan, M.S., Shioda, N., Shibuya, M., Iwabuchi, Y., Fukunaga, K., 2009. Activation of endothelial nitric oxide synthase by a vanadium compound ameliorates pressure overload-induced cardiac injury in ovariectomized rats. Hypertensio 53, 57–63.

Brown, L., Fenning, A., Chan, V., Loch, D., Wilson, K., Anderson, B., Burstow, D., 2002. Echocardiographic assessment of cardiac structure and function in rats. Heart Lung Circ. 11, 167–173.

Caperuto, L.C., Anhê, G.F., Cambiaghi, T.D., Akamine, E.H., do Carmo Buonfiglio, D., Cipolla-Neto, J., Curi, R., Bordin, S., 2008. Modulation of bone morphogenetic protein-9 expression and processing by insulin, glucose, and glucocorticoids: possible candidate for hepatic insulin-sensitizing substance. Endocrinology 149, 6326–6335.

Chen, T.G., Zhong, Z.Y., Sun, G.F., Zhou, Y.X., Zhao, Y., 2011. Effects of tumour necrosis factor-alpha on activity and nitric oxide synthase of endothelial progenitor cells from peripheral blood. Cell Prolif. 44, 352–359.

Chou, T.C., Yen, M.H., Li, C.Y., Ding, Y.A., 1998. Alterations of nitric oxide synthase expression with aging and hypertension in rats. Hypertension 31, 643–648.

Cnop, M., Foufelle, F., Velloso, L.A., 2011. Endoplasmic reticulum stress, obesity and diabetes. Trends Mol. Med. , http://dx.doi.org/10.1016/j.molmed.2011.07.010.

de Alvaro, C., Teruel, T., Hernandez, R., Lorenzo, M., 2004. Tumornecrosis factor alpha produces insulin resistance in skeletal muscle by activation of inhibitor kappaB kinase in a p38 MAPK-dependent manner. J. Biol. Chem. 279, 17070–17078.

DeFronzo, R.A., 2010. Insulin resistance, lipotoxicity, type 2 diabetes and atherosclerosis: the missing links. The Claude Bernard Lecture 2009. Diabetologia 53, 1270–1287.

Desjardins, F., Balligand, J.L., 2006. Nitric oxide-dependent endothelial function and cardiovascular disease. Acta Clin. Belg. 61, 326–334.

Dimmeler, S., Fleming, I., Fisslthaler, B., Hermann, C., Busse, R., Zeiher, A.M., 1999. Activation of nitric oxide synthase in endothelial cells by Akt-dependent phosphorylation. Nature 399, 601–605.

Espinola-Klein, C., Gori, T., Blankenberg, S., Munzel, T., 2011. Inflammatory markers and cardiovascular risk in the metabolic syndrome. Front. Biosci. 16, 1663–1674.

Ha, T., Li, Y., Gao, X., McMullen, J.R., Shioi, T., Izumo, S., Kelley, J.L., Zhao, A., Haddad, G.E., Williams, D.L., Browder, I.W., Kao, R.L., Li, C., 2005. Attenuation of cardiac hypertrophy by inhibiting both mTOR and NFkappaB activation in vivo. Free Radical Biol. Med. 39, 1570–1580.

Kanety, H., Feinstein, R., Papa, M.Z., Hemi, R., Karasik, A., 1995. Tumornecrosis factor alpha-induced phosphorylation of insulin receptor substrate-1 (IRS-1). Possible mechanism for suppression of insulin-stimulated tyrosine phosphorylation of IRS-1. J. Biol. Chem. 270, 23780–23784.

Lee, J.H., Palaia, T., Ragolia, L., 2009. Impaired insulin-mediated vasorelaxation in diabetic Goto-Kakizaki rats is caused by impaired Akt phosphorylation. Am. J. Physiol. Cell. Physiol. 296, C327–C338.

Messer, G., Weiss, E.H., Baeuerle, P.A., 1990. Tumor necrosis factor beta (TNF-beta) induces binding of the NF-kappa B transcription factor to a high-affinity kappa B element in the TNF-beta promoter. Cytokine 2, 389–397.

Paz, K., Hemi, R., LeRoith, D., Karasik, A., Elhanany, E., Kanety, H., Zick, Y., 1997. A molecular basis for insulin resistance. Elevated serine/threonine phosphorylation of IRS-1 and IRS-2 inhibits their binding to the juxtamembrane region of the insulin receptor and impairs their ability to undergo insulin-induced tyrosine phosphorylation. J. Biol. Chem. 272, 29911–29918.

Sanz-Rosa, D., Oubiña, M.P., Cediel, E., de Las Heras, N., Vegazo, O., Jiménez, J., Lahera, V., Cachofeiro, V., 2005. Effect of AT1 receptor antagonism on vascular and circulating inflammatory mediators in SHR: role of NF-kappaB/IkappaB system. Am. J. Physiol. Heart Circ. Physiol. 288, H111–H115.

Scherrer, U., Randin, D., Vollenweider, P., Vollenweider, L., Nicod, P., 1994. Nitric oxide release accounts for insulin's vascular effects in humans. J. Clin. Invest. 94, 2511–2515.

Sugita, M., Sugita, H., Kaneki, M., 2004. Increased insulin receptor substrate 1 serine phosphorylation and stress-activated protein kinase/c-Jun N-terminal kinase activation associated with vascular insulin resistance in spontaneously hypertensive rats. Hypertension 44, 484–489.

Taniguchi, C.M., Emanuelli, B., Kahn, C.R., 2006. Critical nodes in signalling pathways: insights into insulin action. Nat. Rev. Mol. Cell Biol. 7, 85–96.

Tesauro, M., Schinzari, F., Rovella, V., Melina, D., Mores, N., Barini, A., Mettimano, M., Lauro, D., Iantorno, M., Quon, M.J., Cardillo, C., 2008. Tumornecrosis factor-alpha antagonism improves vasodilation during hyperinsulinemia in metabolic syndrome. Diabetes Care 31, 1439–1441.

Virdis, A., Santini, F., Colucci, R., Duranti, E., Salvetti, G., Rugani, I., Segnani, C., Anselmino, M., Bernardini, N., Blandizzi, C., Salvetti, A., Pinchera, A., Taddei, S., 2011. Vascular generation of tumor necrosis factor-α reduces nitric oxide availability in small arteries from visceral fat of obese patients. J. Am. Coll. Cardiol. 58, 238–247.

Watson, L.E., Sheth, M., Denyer, R.F., Dostal, D.E., 2004. Baseline echocardiographic values for adult male rats. J. Am. Soc. Echocardiogr. 17, 161–167.

Yang, J., Park, Y., Zhang, H., Xu, X., Laine, G.A., Dellsperger, K.C., Zhang, C., 2009. Feed-forward signaling of TNF-alpha and NF-kappaB via IKK-beta pathway contributes to insulin resistance and coronary arteriolar dysfunction in type 2 diabetic mice. Am. J. Physiol. Heart Circ. Physiol. 296, H1850–H1858.

Yang, X.P., Liu, Y.H., Shesely, E.G., Bulagannawar, M., Liu, F., Carretero, O.A., 1999. Endothelial nitric oxide gene knockout mice: cardiac phenotypes and the effect of angiotensin-converting enzyme inhibitor on myocardial ischemia/reperfusion injury. Hypertension 34, 24–30.

Zecchin, H.G., Bezerra, R.M., Carvalheira, J.B., Carvalho-Filho, M.A., Metze, K., Franchini, K.G., Saad, M.J., 2003. Insulin signalling pathways in aorta and muscle from two animal models of insulin resistance–the obese middle-aged and the spontaneously hypertensive rats. Diabetologia 46, 479–491.

Zeng, G., Nystrom, F.H., Ravichandran, L.V., Cong, L.N., Kirby, M., Mostowski, H., Quon, M.J., 2000. Roles for insulin receptor, PI3-kinase, and Akt in insulin-signaling pathways related to production of nitric oxide in human vascular endothelial cells. Circulation 101, 1539–1545.